CRYSTAL GROWTH & DESIGN
2006
VOL. 6, NO. 11
2598−2602

Characterization of a 3C-SiC Single Domain Grown on 6H-SiC(0001) by a Vapor−Liquid−Solid Mechanism

Maher Soueidan,*,†,‡ Gabriel Ferro,† Bilal Nsouli,‡ Mohamad Roumie,‡ Efstathios Polychroniadis,§ Michel Kazan,⊥ Sandrine Juillaguet,⊥ Didier Chaussende,∥ Nada Habka,† John Stoemenos,§ Jean Camassel,⊥ and Yves Monteil†

Laboratoire des Multimatériaux et Interfaces, UMR-CNRS 5615, Bât. Berthollet, Université Claude Bernard Lyon 1, 43 Bd du 11 Novembre 1918, 69622 Villeurbanne Cedex, France, Lebanese Atomic Energy Commission-CNRS, P.O. Box 11-8281, Riad El Solh, 1107 2260 Beirut, Lebanon, Physics Department, Aristotle University of Thessaloniki, GR 54124 Thessaloniki, Greece, Groupe d'Etude des Semiconducteurs, UMR-CNRS 5650, Université Montpellier 2, cc074, 34095 Montpellier Cedex 5, France, and INPGrenoble-CNRS, 961 rue de la Houille Blanche, BP 46, 38402 St Martin d'Hères, France

Received June 12, 2006; Revised Manuscript Received August 23, 2006

ABSTRACT: By a vapor−liquid−solid (VLS) mechanism, where a Ge−Si melt is fed by propane, 3C-SiC layers of ~1.4 μm thickness were grown on 6H-SiC on-axis substrates. These layers were found to be single domain as seen from morphological and electron backscattering diffraction observations. They were free of any hexagonal inclusion. Both transmission electron microscopy and high-resolution X-ray diffraction show the high crystalline quality of the grown material. Nitrogen was found to be the main impurity, at a concentration of (6−7) $\times$ 10^{17} cm^{-3} as estimated by Raman spectroscopy, though Al contamination was also detected by low-temperature photoluminescence. The identification and the quantification of Ge incorporation inside the SiC layers were determined by particle-induced X-ray emission (PIXE). The Ge concentration was calculated to be 5 $\times$ 10^{18} atoms/cm^3.

Introduction

Silicon carbide (SiC) is a suitable semiconductor material for high-temperature, high-power, and high-frequency electronic devices, because of its wide band gap, high electron mobility and high electron saturation velocity. Among the long list of SiC polytypes identified, large area commercially available wafers are mainly of the 6H and 4H polytypes. The only cubic phase, noted 3C or β, has specific advantages over the hexagonal forms, which make it desirable for device applications. For instance, 3C-SiC might help increase the channel mobility of a metal oxide semiconductor (MOS)−SiC device.[1] Its smaller band gap may also reduce the electric field strength required to achieve channel inversion.

A 3C-SiC crystal can be grown on a Si substrate by chemical vapor deposition (CVD).[2] But major problems are encountered in this heteroepitaxial system such as the large lattice mismatch of 20% and the difference in the thermal expansion coefficients of 8% between SiC and Si. Recently, Nagasawa et al. developed 100 mm free-standing 3C-SiC(100) crystals with good crystallinity using undulant Si substrate and high growth rates.[3]

3C-SiC(111) material can also be heteroepitaxially grown on 6H-SiC(0001) on axis substrate either by CVD[4] or by sublimation.[5] In that heteroepitaxial system, the lattice and thermal mismatch between the seed and the layer is almost negligible, so higher quality layers are expected to be obtained. However, another type of defect, called double positioning boundary (DPB), forms in these 3C-SiC layers due to a 60° rotation of the initial 3C stacking on the (0001) hexagonal plane, each orientation having equivalent probability of nucleation. If inappropriate conditions are used, the 3C-SiC layers on 6H-SiC contains a high density of DPBs.[6] Xie et al. pointed out the importance of in situ surface preparation of the commercial substrate before CVD growth for DPB density reduction.[7] It was also suggested that low defect density 3C-SiC layers are difficult to achieve because it may compete with the formation of homoepitaxial layers by step-controlled epitaxy. An interesting approach was proposed by Neudeck et al., in which 0.2 $\times$ 0.2 mm^2 mesas were used to produce step-free surfaces and to locally grow 3C-SiC material without DPBs.[8] However, the local presence of screw dislocations reduces the yield of fabrication of these step-free mesas. Furthermore, growth of homogeneous 3C-SiC layers on the whole substrate surface would be more suited for further uses such as device processing or even as seed for bulk growth.

Beside these well-known techniques (CVD and sublimation), new growth approaches may also bring innovating results. For instance, continuous feed physical vapor transport (CF-PVT), which uses basically a sublimation chamber fed continuously by precursor gases, has already produced 400 μm thick single-domain 3C-SiC material over a 30 mm diameter.[9] However, CF-PVT is a high-temperature process where the fine control of the initial nucleation is difficult. Furthermore, this high temperature may favor the generation of stacking fault since the energy of formation of this defect was found to be negative in 3C-SiC polytype.[10]

The only references to 3C-SiC formation from the melt on α-SiC substrate can be found in works of Tanaka et al.[11,12] But in that case, the growth technique was not standard since the Al−Si-based melts were fed with propane at 1000 °C to grow the SiC layers. It can thus be considered as a vapor−solid−liquid (VLS) mechanism. These 3C-SiC grown layers were obviously not single domain because they displayed triangular features with 60° rotation. Using a VLS mechanism in Ge−Si melts, some of the present authors have already demonstrated the possibility to obtain large area 3C-SiC single-domain layers.[13] Characterizations of these layers are presented here using a wide spectrum of techniques.

* Corresponding author. E-mail: maher.soueidan@univ-lyon1.fr. Tel: +33 4 72 43 82 31. Fax: +33 4 72 44 06 18.
† Université Claude Bernard Lyon 1.
‡ Lebanese Atomic Energy Commission-CNRS.
§ Aristotle University of Thessaloniki.
⊥ Université Montpellier 2.
∥ INPGrenoble-CNRS.

10.1021/cg0603523 CCC: $33.50 © 2006 American Chemical Society
Published on Web 10/07/2006

Experimental Section

The experiments were carried out in homemade epitaxy equipment working at atmospheric pressure. For further details on the experimental set up, one can see refs 13 and 14. Briefly, the 6H-SiC(0001) on-axis Si face seeds were placed at the bottom of a graphite crucible. Si and Ge pieces were then stacked on top of the seed and heated under purified Ar up to 1200−1450 °C in order to form a liquid containing 25 atom % Si. Propane was added at high temperature to start SiC growth by the VLS mechanism. Before cooling at the end of the experiment, the liquid was sucked out, leaving some small traces of remaining alloy, which were eliminated by wet chemical etching in $HCl-HF-HNO_3$ solution.

The grown layers were characterized by different means. For morphological observation, Nomarski optical microscopy was sufficient because the layers are highly step bunched. Complementary information was obtained using electron backscattering diffraction (EBSD) for surface mapping of the grown polytype, with the possibility of separating areas with different orientation such as on each side of a DPB.[15,16] This imaging was performed with a TSL (TexSEM Lab.) system installed on a JEOL 840A scanning electron microscope with the Orientation Imaging Microscopy software.

The 3C-SiC single-domain layers were also characterized by different optical techniques. Polytype identification was routinely performed by micro-Raman spectroscopy using an Ar laser beam (λ = 488 nm) focused to obtain a spot of few square micrometers. Though a confocal configuration was used, contribution from the substrate was difficult to eliminate completely. Doping information can also be extracted from these Raman spectra as described later. Photoluminescence measurements were carried out at low temperature (5 K) in a closed He-cycle cryostat using the 350 nm line of an argon ion laser as excitation source (laser power up to 200 mW) and a 0.6 m spectrometer equipped with a photomultiplier tube detector. Infrared reflectivity spectra were taken in a vacuum at room temperature in the 400−7500 cm^{-1} frequency range using a Bruker IFS 66V spectrometer. A KBr beam splitter and a DTGS detector with a resolution of less than 1 cm^{-1} were used. The light was nonpolarized and at near-normal incidence. The obtained reflectivity was compared with that of a gold-coated mirror with an assumed reflectance of 0.98.

Structural investigations were carried out by high-resolution X-ray diffraction (HRXRD) measurements and transmission electron microscopy (TEM) observations. The former technique was performed in a Philips high-resolution diffractometer with Cu Kα radiation and a spot size of 0.8 × 0.8 mm^2. The sample was positioned in an Eulerian cradle, where position optimization of the scattering vector was facilitated by independent variation of the incident angle (ω) and the diffraction angle (2θ). A double monochromator was used with a resolution of <0.01°. The cross-section TEM was performed on a JEM 100CX instrument operating at 100 keV. The samples were prepared in an ion milling instrument equipped with a liquid nitrogen cold trap and operated at a gun voltage of 4 kV with an incident angle of 5°. Prior to milling, the samples were mechanically thinned down to 20 μm.

Elementary analyses were performed using a particle-induced X-ray emission (PIXE) technique in order to detect Ge incorporation inside the layer. This technique is multielemental, nondestructive, and sensitive with a limit of detection down to the ppm level.[17] The 1.7 MV tandem accelerator of the Lebanese Atomic Energy Commission[18] was used to deliver a proton beam of 1 MeV energy on the samples with 245 μC of fluence. This fluence was enough to have less than 5% of statistical error in the measured peak area for Ge. To attenuate the high count rate of the Si signal, emitted from both the substrate and the film, a Kapton filter of 260 μm thickness was used as X-ray absorber and placed in front of the Si(Li) X-ray detector. The X-ray spectra were, in off-line mode, analyzed with the GUPIX computer code.[19] This allows quantification of the Ge content in the layer.

Results and Discussion

Typical surface morphologies of layers grown by VLS are shown in Figure 1a,b. Micro-Raman spectroscopy performed on such layers displayed a strong TO peak at 796 cm^{-1}, which is the fingerprint of the 3C-SiC polytype (Figure 2). EBSD orientation and phase mapping confirmed the absence of either other polytype inclusions or areas with 60° rotated orientation (see ref 13 for illustration). The grown material is thus single domain, that is, without any DPBs. It is, in fact, very easy to detect and locate the DPBs inside the layers by simply observing the morphology. Indeed, on each side of this defect, the tips of the step front show evidence of 60° rotation as shown in Figure 1c. This is due to a 60° rotation of the 3C-SiC material, which modifies the step faceting. As a consequence, the simple observation of the surface morphology is sufficient to determine whether the layer is single domain.

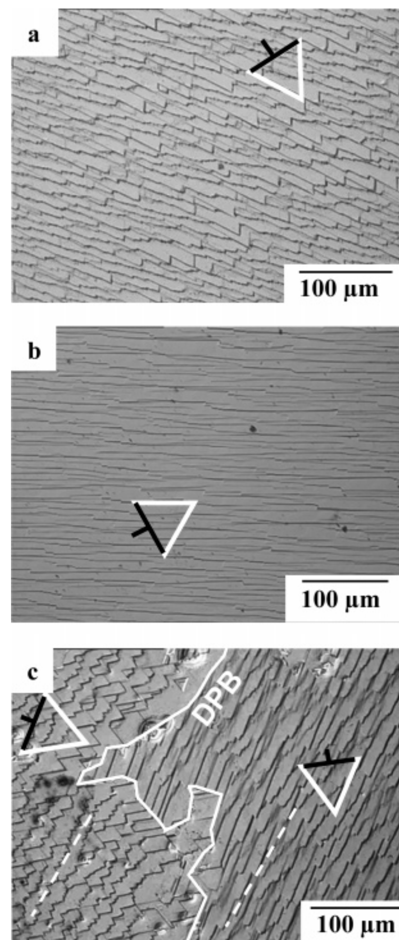

Figure 1. (a, b) Two main kinds of surface morphology observed on single-domain 3C-SiC layers grown by VLS in Si−Ge melt and (c) morphology of a two-domain layer on each side of a DPB. The dashed lines indicate the step front orientation. The triangles indicate the tips orientation of the step front and illustrate the local orientation of the 3C-SiC layer.

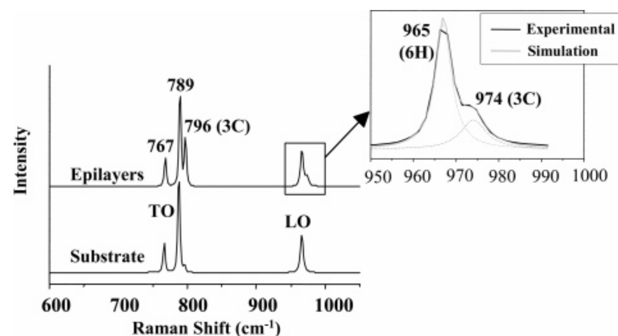

Figure 2. Micro-Raman spectra collected on a 6H-SiC substrate and a single-domain 3C-SiC epilayer. The spectrum at the LO mode position was simulated to extract the doping level.

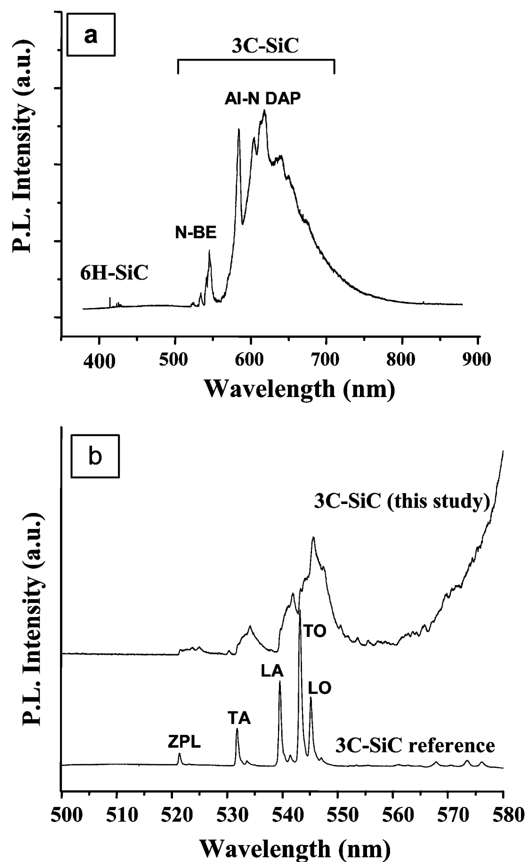

Figure 3. LTPL spectrum collected at 5 K on a 3C-SiC single-domain layer grown by VLS in this work: (a) complete spectrum and (b) zoom on the N-BE bands compared with the one of a reference 3C-SiC bulk sample.

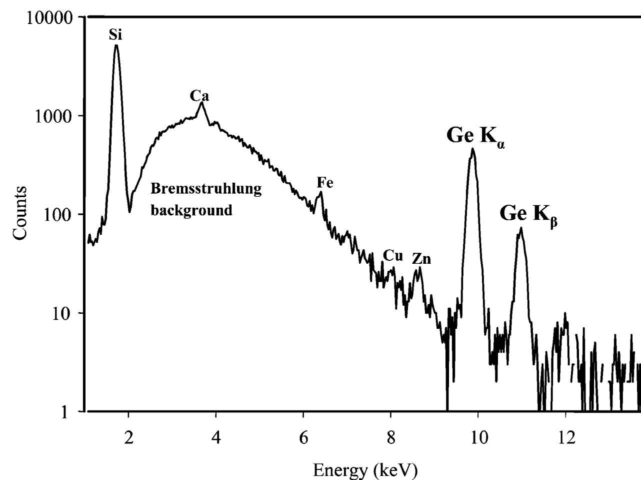

Figure 4. PIXE spectrum of the SiC (Ge)/SiC using 1 MeV energy of proton beam with 245 μC of fluence.

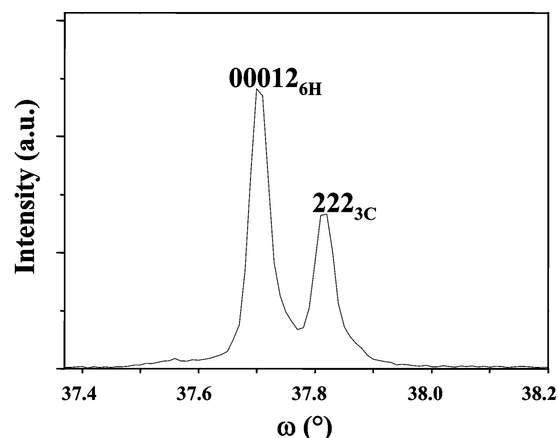

Figure 5. HRXRD spectrum of a 3C-SiC single-domain layer grown on 6H-SiC by VLS in Si−Ge melt.

Raman spectroscopy was also used to evaluate the doping level of the 3C-SiC layers. Indeed, the position and shape of the LO peak is known to be n-type doping dependent, allowing quantitative calibration.[20] On our layers, the 3C-SiC LO peak was shifted from 972 cm^{-1} (low doped material) to 974 cm^{-1} and its full width at half-maximum (FWHM) was 10 cm^{-1} (see Figure 2). With these values, the residual n-type doping was estimated to be $(6-7) \times 10^{17}$ cm^{-3}. The source of this doping may be the nitrogen impurity present in the gases (30 ppm for propane and 10 ppm for Ar).

This nitrogen doping was also detected by low-temperature photoluminescence (LTPL) (Figure 3a). 3C-SiC related emission is observed above 500 nm with broad nitrogen bound exciton (N-BE) bands between 520 and 550 nm. Strong Al−N donor−acceptor pair (DAP) transitions are also detected around 620 nm. The Al contamination may come from the graphite of the crucible or more probably from the graphite glue used to fix the seed at the bottom of the crucible since the raw material used for this glue is not of semiconductor-grade purity. The LTPL spectrum of Figure 3 shows also some small contribution from the substrate at higher energy.

Figure 4 shows the PIXE spectrum of the identically grown single-domain layer. One can easily see the Ge-related signals (K_α and K_β peaks), far from the huge Bremsstrahlung background. Assuming a layer thickness of 1.4 μm, the Ge concentration was found to be 0.0235 wt % corresponding to $(5 \pm 0.2) \times 10^{18}$ atoms/cm^3 in the SiC layer. Other elements than Ge were also detected by PIXE, that is, Ca, Fe, Cu, and Zn. While the Ca can be attributed to surface contamination to air, after growth, the other metallic elements can either come from identical surface contamination or from the growth system (the liquid or the crucible). Assuming a contamination during growth, the concentration inside the 3C-SiC layer was found to be 23 ± 2 ppm for Fe, 17 ± 2 ppm for Cu, and 76 ± 3 ppm for Zn. Investigations are underway to check the exact origin of these elements.

Coming back to the N-BE bands, a zoom on this spectral zone displayed in Figure 3b shows that these peaks are broadened and shifted toward lower energy compared with bulk reference 3C-SiC material. This red shift seems to be constant and approximately of 14 meV. Since the doping level determined by Raman spectroscopy is not sufficient to explain it, the origin may be different. One can suggest that the Ge content inside the layer, as determined by PIXE, may affect its optical properties. Strain due to lattice mismatch between the substrate and the layer can also be considered since this mismatch is not negligible (0.09%). Note that this theoretical strain should be tension. Assuming a tetragonal distortion of the lattice, a tensile strain should involve a red shift of the PL peaks.[21] This is the case here. Of course, Ge incorporation and tensile strain can have cumulative effects on the optical properties of the grown layers.

This small mismatch allows also separation of the XRD (0001) and (111) family peaks coming from the substrate and the layer, respectively (Figure 5). The FWHM of these peaks, as obtained from the HRXRD rocking curve taken on a single-domain 3C-SiC layer grown in this study, display very similar

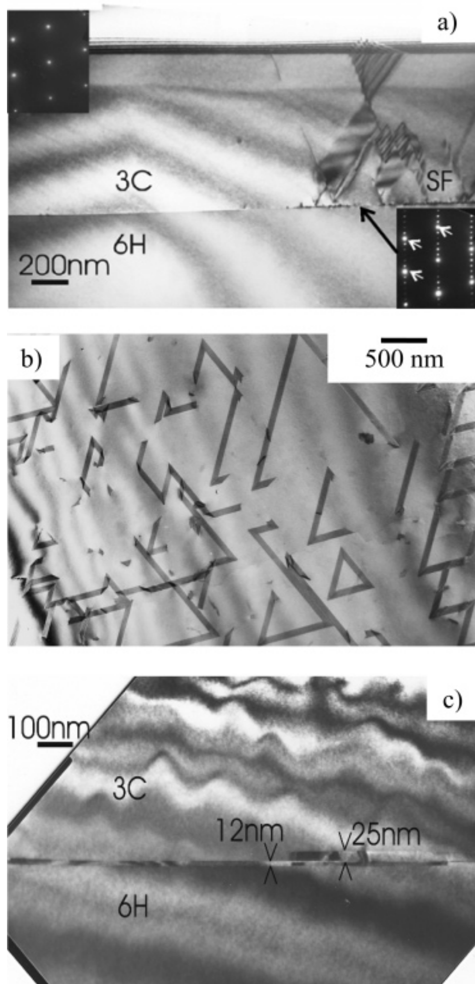

Figure 6. (a) Cross sectional TEM micrograph of a single-domain 3C-SiC layer. The only defects are some SFs emanating from the 3C/6H interface. The corresponding diffraction pattern from the 3C-SiC overgrown is shown in the inset in the left side upper corner. The superimposed 3C and 6H diffraction patterns taken from the 3C/6H interface are evident in the inset in the right side corner. (b) Plan view TEM micrograph taken from the uppermost part of the 3C-SiC film. The only defects at the surface are SFs. (c) Cross sectional TEM micrograph taken at the 3C/6H interface. Very thin slabs of DPBs are evident at the interface.

values between the substrate and the epilayer, 126.37 and 138.40 arcsec, respectively. This indicates that the crystalline quality of the 3C-SiC layer is very good, far better than for the layers grown on Si substrates.

Cross-sectional TEM investigations did not evidence any DPB inside the layer in the investigated areas (Figure 6). The only defects found were stacking faults (SFs), which formed at the interface and propagated through the layer. Their density was estimated to be 4×10^3 cm^{-1} by plan view TEM (Figure 6b). These defects form triangular features due to the 3-fold symmetry of the 3C-SiC crystal along the (111) direction. The thickness of the 3C-SiC layer was estimated to be 1.4 μm.

Rarely very thin DPBs were observed near and parallel to the substrate/epilayer interface, as shown in Figure 6. These DPBs are (111) twins having their twin plane perpendicular to the [111] direction of growth. No inclined twins were formed on the other equivalent {111} planes. It is obvious from Figure 6 that the single-domain layer completely overgrew these inclusions. This suggests that the obtaining of a single-domain layer does not necessarily imply an initial single-domain nucleation but the mechanism can accept the initial formation of two domains followed by a rapid lateral overgrowth of the minority domain by the majority one. The reason for this is still unknown, but the results are reproducible. A systematic observation of the step tip rotation compared with the average step direction may help determine the planes with faster growth rate and thus the mechanism of domain selection. This work is in progress.

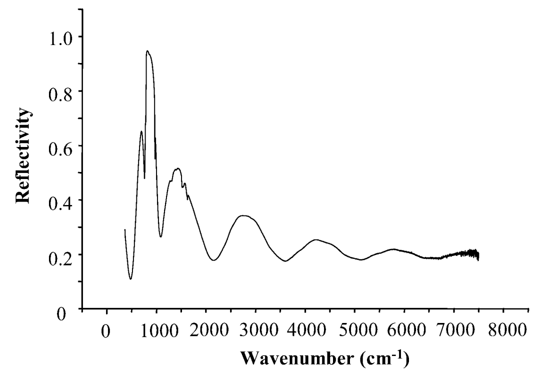

Figure 7. FTIR spectrum of a 3C-SiC layer grown in this study.

The FTIR reflectivity spectrum collected from a single-domain layer shows the strong Restrahlen band of SiC and several oscillations, which attenuate at high wavenumber values (Figure 7). These oscillations are due to a slight difference in refractive index between the substrate and the layer giving rise to multiple reflections inside the 3C-SiC layer. The thickness D can then be deduced using the equation

$$D = 1/(2n\Delta\nu) \tag{1}$$

where n is the ordinary refractive index of the layer (2.54) and $\Delta\nu$ is the oscillation period. A thickness of 1.34 μm was obtained, which is very close to the one measured by TEM.

Conclusion

Single-domain 3C-SiC layers grown by VLS in Ge−Si melt were characterized by several means. Morphological, optical, and structural investigations confirmed the high crystalline quality of this material. Ge was found to incorporate inside the layers in a non-negligible level. The question is whether this will affect the electronic properties of the grown material. Electrical measurements are under way to check this effect and to confirm the potential of such layers.

Acknowledgment. M.S. and N.H. gratefully acknowledge the financial support from the Lebanese National Council for Scientific Research (CNRSL). Authors acknowledge the financial support provided by the Lebanese−French CEDRE research program and thank the CECOMO of Lyon for the Micro-Raman measurements.

References

(1) Lu, C. Y.; Cooper Jr, J. A.; Chung, G. Y.; Williams, J. R.; McDonald, K.; Feldman, L. C. *Mater. Sci. Forum* **2002**, *389−393*, 977.
(2) Nishino, S.; Powell, J. A.; Will, H. A. *Appl. Phys. Lett.* **1983**, *42*, 460.
(3) Nagazawa, H.; Yagi, K.; Kawahara, T. *J. Cryst. Growth* **2002**, *237−239*, 1244.
(4) Powell, J. A.; Larkin, D. J.; Matus, L. G.; Choyke, W. J.; Bradshaw, J. L.; Henderson, L.; Yoganathan, M.; Yang, J.; Pirouz, P. *Appl. Phys. Lett.* **1990**, *56*, 1353.
(5) Andreev, A. N.; Tregubova, A. S.; Scheglov, M. P.; Syrkin, A. L.; Chelnokov, V. E. *Mater. Sci. Eng. B* **1997**, *46*, 141.

(6) Soueidan, M.; Ferro, G.; Dazord, J.; Monteil, Y.; Younes, G. *J. Cryst. Growth* **2005**, *275* (1−2), 1011.
(7) Xie, Z. Y.; Edgar, J. H.; Burkland, B. K.; George, J. T.; Chaudhuri, J. *J. Cryst. Growth* **2001**, *224*, 235.
(8) Neudeck, P. G.; Powell, J. A. In *Recent Major Advances in SiC*; Choyke, W. J., Matsunami, H., Pensel, G., Eds.; Springer-Verlag: Heidelberg, Germany, 2003; pp 179−205.
(9) Chaussende, D.; Latu-Romain, L.; Auvray, L.; Ucar, M.; Pons, M.; Madar, R.; *Mater. Sci. Forum* **2005**, *483*−*485*, 225.
(10) Lindefelt, U.; Iwata, H.; Oberg, S.; Briddon, P. R. *Phys. Rev. B* **2003**, *67*, No. 155204.
(11) Tanaka, A.; Shiozaki, N.; Katsuno, H. *J. Cryst. Growth* **2002**, *237*−*239*, 1202.
(12) Tanaka, A.; Ataka, A.; Ohkura, E.; Katsuno, H. *J. Cryst. Growth* **2004**, *269*, 413.
(13) Soueidan, M.; Ferro, G. *Adv. Funct. Mater*. **2006**, *16*, 975.
(14) Ferro, G.; Jacquier, C. *New J. Chem*. **2004**, *28* (8), 889−896.
(15) Schwartz, A. J.; Kumar, M.; Adams, B. L. *Electron Backscatter Diffraction in Materials Science*; Kluwer Academic/Plenum Publishers: New York, 2000.
(16) Chaussende, D.; Chaudouet, P.; Auvray, L.; Pons, M.; Madar, R. *Mater. Sci. Forum* **2004**, *457*−*460*, 387.
(17) Johansson, S. A. E.; Campbell, J. L. *Particle-Induced X-ray Emission Spectrometry (PIXE)*; John Wiley & Sons: New York, 1995.
(18) Roumié, M.; Nsouli, B.; Zahraman, K.; Reslan, A. *Nucl. Instrum. Methods B* **2004**, *219*−*220*, 389.
(19) Maxwell, J. A.; Campbell, J. A.; Teesdale, W. J. *Nucl. Instrum. Methods B* **1989**, *43*, 218.
(20) Nakashima, S.; Harima, H. *Phys. Status Solidi a* **1997**, *162*, 39.
(21) Pikus, G. E.; Bir, G. L. *Sov. Phys. Solid State* **1960**, *1*, 1502.

CG0603523